Stochastic Loss in Dielectric Slab Waveguides due to Exponential and Uncorrelated Surface Roughness

Brian Guiana and Ata Zadehgol
University of Idaho, Moscow, ID 83844, USA
bguiana@uidaho.edu, azadehgol@uidaho.edu

***Abstract*—In this work we analyze the stochastic scattering loss in silicon-on-insulator (Si/SiO_2) waveguides represented by symmetric dielectric slab waveguides exhibiting exponential and uncorrelated surface roughness, operating in the transverse electric mode at optical frequencies (wavelength $\lambda = 1.54$ μm). We use the finite-difference time-domain (FDTD) method to simulate hundreds of rough waveguides, and compare those results with loss from previously established planar analytical equations by [1]. The data and analysis point to a modification of the loss equation in [1], [3] that reduces the error in scattering loss between the analytical equation and the FDTD simulations by up to approx 30%.**

I. Introduction

Silicon-on-insulator (SOI) technology is an important component of integrated circuit technologies, where ultra-small form-factors and ultra-high operating frequencies are increasingly common. Fabricating and testing hardware can be cost-prohibitive, but computer simulation can be utilized as a cost-effective predictive tool for modeling system behavior. In this paper, we propose a modification to an existing equation [1], [3] for modeling stochastic scattering loss in dielectric slab waveguides (DSWs) exhibiting surface roughness with an *exponential* autocorrelation. We use the FDTD method, adapted to the two-dimensional transverse electric (TE) mode, to simulate hundreds of DSWs exhibiting stochastic surface roughness, where the roughness profiles on the boundaries between Si (core) and SiO_2 (cladding) regions are *uncorrelated*. We discuss the simulation results and discuss the differences.

II. Formulation

The general formulation for scattering loss can be found by taking the ratio of power radiated from the DSW (P_{rad}) and power guided through it (P_g). Using the corresponding equations from [1], the scattering loss α (Np/m) can then be calculated with (1) [1]–[3].

$$\alpha = \frac{\eta_g}{\eta_{\text{rad}}} \frac{\cos^2(\kappa d)}{d + \frac{1}{\gamma}} \left(n_1^2 - n_2^2\right)^2 \frac{k_0^3}{4\pi n_2} \int_0^\pi \tilde{R}(k_\theta) d\theta, \qquad (1)$$

where d (m) is the half-width of the DSW, n_1 is the refractive index of the core region, n_2 is the refractive index of the cladding region, η_g (Ω) is the intrinsic impedance of P_g, η_{rad} (Ω) is the intrinsic impedance of P_{rad}, k_0 is the free-space wave number, $\kappa = \sqrt{n_1^2 k_0^2 - \beta^2}$, $\gamma = \sqrt{\beta^2 - n_2^2 k_0^2}$, and β (m^{-1}) is the propagation constant found via the effective index method [3]. The term $R(\zeta)$ is the ideal autocorrelation function (ACF) for the waveguide roughness profile, and $\tilde{R}(k)$ is the spatial Fourier transform of $R(\zeta)$, where the input $k_\theta = \beta - n_2 k_0 \cos\theta$. We use the exponential ACF, where $R(\zeta) = \sigma^2 \exp(-|\zeta|/L_c)$, σ is the profile standard deviation, and L_c is the correlation length. The geometry and field orientation are identical to those described in [2], but the simulation methodology now involves generating unique roughness profiles for *both* boundaries between core and cladding regions, rather than generating only one roughness profile and applying it to both boundaries.

The formulation presented by [1] assumes $\eta_{\text{rad}} = \frac{\eta_0}{n_2}$ and $\eta_g = \frac{\eta_0}{n_1}$, where η_0 is the intrinsic impedance of free-space. We can see by inspection that the $\eta_{\text{rad}} = \frac{\eta_0}{n_2}$ can be assumed true. However, evaluating P_g with the Poynting vector calculated from the field components (56) and (60) in [3] shows that $\eta_g = \frac{\omega\mu_0}{\beta} = \frac{\eta_0}{n_{\text{eff}}}$ should be used, where ω is the angular frequency and μ_0 is the vacuum magnetic permeability.

III. Results and Discussion

We use the same discretization for FDTD simulations as was used in [2]. Unless otherwise stated the refractive indices are $n_1 = 3.5$ and $n_2 = 1.5$, the source frequency is $f_0 = 194.8$ THz, the length of the waveguide is 20 μm, the nominal width is $2d = 100$ nm, and $\eta_{\text{rad}} = \frac{\eta_0}{n_2}$.

A. Guided Power

We compare the power distribution across the width of the DSW in Fig. 1, where the combination of (56) and (60) from [3] is compared with two forms of FDTD simulation results. Form 1 uses the E-field magnitude squared and the effective impedance, and form 2 uses the E-field and H-field.

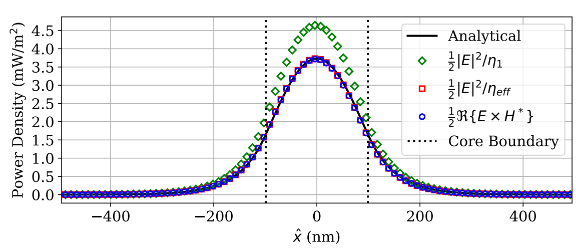

Fig. 1. Power density distribution across the DSW width. Diamond is form 1 with $\eta_g = \frac{\eta_0}{n_1}$. Square is form 1 with $\eta_g = \frac{\eta_0}{n_{\text{eff}}}$. Circle is form 2. $\Re\{x\}$ is the real part of x.

Figure 1 compares power density evaluated from FDTD simulation and analytical power density distribution. To quantify the closeness of FDTD results to the analytical equation, we numerically integrate the FDTD results across the DSW width and compare those with the integral of the analytical equation. We calculate the error with $E_p = 100|(\mathrm{F} - \mathrm{A})/\mathrm{F}|$, where A is the analytical equation and F is the corresponding FDTD result. For F being form 1 with $\eta_g = \frac{\eta_0}{n_{\text{eff}}}$, $E_p \approx 0.3\%$, for F being form 1 with $\eta_g = \frac{\eta_0}{n_1}$, $E_p \approx 19.4\%$, and for F being form 2, $E_p \approx 0.6\%$. This comparison shows that form 1 with the assumption $\eta_g = \frac{\eta_0}{n_{\text{eff}}}$ and form 2 both result in a very small error. Whereas form 1 with $\eta_g = \frac{\eta_0}{n_1}$ results in a large error. Such a small error shows that using $\eta_g = \frac{\eta_0}{n_{\text{eff}}}$ is the most accurate method for calculating P_g in the DSW.

B. Scattering Loss Comparisons

We simulated DSWs with roughness profiles over a range of σ and L_c values. Each simulation generates unique roughness profiles for both the upper and the lower core/cladding boundaries. The simulation setups are each combination of $\sigma \in \{9, 15\}$ nm and $L_c \in \{200, 300, ..., 1000\}$ nm. 2168 waveguides were simulated (about 120 simulations per setup). We control for potential mismatch between simulation results and (1) by evaluating σ and L_c for each roughness profile in that set, followed by taking the mean those σ and L_c values, and using those in (1); a detailed explanation is provided in [2]. The error for each setup is calculated using (2).

$$\%E = 100 \times \frac{\alpha_{\text{analytical}} - \bar{\alpha}_{\text{simulation}}}{\alpha_{\text{analytical}}}, \qquad (2)$$

where $\alpha_{\text{analytical}}$ is (1) and $\bar{\alpha}_{\text{simulation}}$ is the mean scattering loss calculated from FDTD results with the corresponding setup.

We use the assumption $\eta_g = \frac{\eta_0}{n_1}$ according to [1] to calculate the error between (1) and simulation results, and we show those errors in Fig. 2. We observe that 10 of the 18 setups have errors with magnitudes larger than 30%. This results in the average error being between -30% and -40%, where (1) underestimates the FDTD scattering loss for each setup.

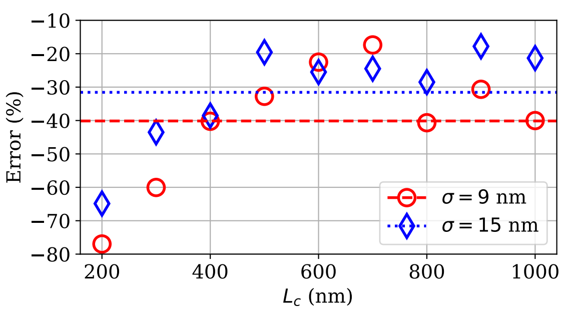

Fig. 2. Percentage error for FDTD simulation results compared with (1), where $\eta_g = \frac{\eta_0}{n_1}$, according to [1]. Markers show setup error. Lines show mean error for each σ.

Next, we use the assumption $\eta_g = \frac{\eta_0}{n_{\text{eff}}}$ according to [3] to perform a similar error comparison between (1) and simulation results in Fig. 3. With this assumption, η_g is effectively a scaling factor, so the errors for each setup are similar in layout, but the errors themselves have been reduced significantly. Equation (1) still underestimates the evaluated simulation scattering loss, but not to the same extent as with $\eta_g = \frac{\eta_0}{n_1}$. Now, 10 of the 18 setups have errors with magnitudes smaller than 10%, and the average error is between -5% and -10%.

In Figs. 2 and 3, the errors from simulations with $\sigma = 9$ nm generally have a larger magnitude than those from $\sigma = 15$ nm, and as L_c increases the errors appear to approach a range of values. These observations are likely due to the particular FDTD discretization used.

In [2] it was shown that the assumption $\eta_g = \frac{\eta_0}{n_1}$ results in a very small error, but here we show that the same assumption and comparison results in a much larger error. This is because the simulations in [2] used *correlated* roughness profiles, i.e., the profile on the lower boundary is a direct copy of the profile generated for the upper boundary, whereas here the simulations use *uncorrelated* profiles, i.e., a unique profile is generated for both boundaries.

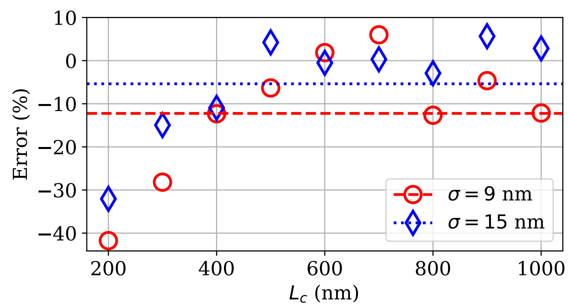

Fig. 3. Percentage error for FDTD simulation results compared with (1), where $\eta_g = \frac{\eta_0}{n_{\text{eff}}}$ according to [3].

IV. Conclusion

The data and analysis in this work showed that the term $\eta_g = \frac{\eta_0}{n_{\text{eff}}}$ from [3] (instead of $\eta_g = \frac{\eta_0}{n_1}$ from [1]) offers a more accurate match to the FDTD results (by up to approximately 30%), for the TE mode stochastic scattering loss experienced by a guided wave in a DSW with uncorrelated roughness profiles. Hundreds of rough waveguides were simulated in FDTD [4] to compare the two assumptions for (1). Work is currently underway to expand this methodology to the *transverse magnetic* (TM) modes.

References

[1] J. Lacey and F. Payne, "Radiation loss from planar waveguides with random wall imperfections," in *IEE Proceedings*, vol. 137, no. 4, 1990, pp. 282–288.

[2] B. Guiana and A. Zadehgol, "Characterizing THz Scattering Loss in Nano-Scale SOI Waveguides Exhibiting Stochastic Surface Roughness with Exponential Autocorrelation," *Electronics*, vol. 11, no. 3, 2022. [Online]. Available: https://www.mdpi.com/2079-9292/11/3/307

[3] A. Zadehgol, "Complex s-plane modeling and 2d characterization of the stochastic scattering loss in symmetric dielectric slab waveguides exhibiting ergodic surface-roughness with an exponential autocorrelation function," *IEEE Access*, vol. 9, pp. 92 326–92 344, 2021.

[4] B. Guiana, "Optical Interconnect Designer Tool (OIDT)." https://github.com/bmguiana/OIDT, created on November 23, 2021.

[5] "GNU General Public License v3.0," https://www.gnu.org/licenses/gpl-3.0.en.html, accessed: Oct. 20, 2021.